Dendrochronologia 88 (2024) 126267

Contents lists available at ScienceDirect

Dendrochronologia

journal homepage: www.elsevier.com/locate/dendro

Tree-ring blue intensity measurements from treeline sites in the Ural Mountains exhibit a strong summer temperature signal

Viktoria V. Agapova [a], Alberto Arzac [a,*], Vladimir V. Kukarskih [a,b], Ulf Büntgen [c,d,e,f], Jan Esper [e,g], Alexander V. Kirdyanov [a,c,h]

[a] *Siberian Federal University, Krasnoyarsk, Russia*
[b] *Institute of Plant and Animal Ecology, Ural Branch, Russian Academy of Sciences, Yekaterinburg, Russia*
[c] *Department of Geography, University of Cambridge, Cambridge, UK*
[d] *Swiss Federal Research Institute (WSL), Birmensdorf, Switzerland*
[e] *Global Change Research Centre, Czech Academy of Sciences, Brno, Czech Republic*
[f] *Department of Geography, Faculty of Science, Masaryk University, Brno, Czech Republic*
[g] *Department of Geography, Johannes Gutenberg University, Mainz, Germany*
[h] *V.N. Sukachev Institute of Forest SB RAS, Federal Research Center "Krasnoyarsk Science Center SB RAS", Krasnoyarsk, Russia*

A R T I C L E I N F O

Keywords:
Climate change
Earlywood
Larix sibirica
Latewood
Tree-ring width
Wood density

A B S T R A C T

The high northern latitudes offer an ideal environment to analyze tree growth responses to unprecedented recent warming. In this study, for the first time, we explore the dendroclimatological potential of latewood blue intensity (LWBI) and delta blue intensity (DBI) at two Siberian larch (*Larix sibirica* Ledeb.) sites in the upper treeline ecotone of the Ural Mountains, northern Russia. To assess the climate signals encoded in LWBI and DBI, as well as tree-ring width (TRW) and maximum latewood density (MXD), we correlated these parameter-specific chronologies against monthly temperature means, precipitation totals, and the SPEI index. LWBI and BDI exhibit robust and stable positive correlations with summer temperature, higher than TRW but slightly lower than MXD at both sites, with marginal negative effects from precipitation and strong negative correlations with SPEI. As direct surrogates for MXD, LWBI and DBI from larch trees offer reasonable alternatives as proxies for temperatures in northern latitudes.

1. Introduction

Treelines are temperature-limited environments (Harsch et al., 2009; Körner, 2012; Körner and Paulsen, 2004; Paulsen and Körner, 2014; Shyatov, 1986), where short growing seasons limit carbon assimilation (MacDonald et al., 2008). Global warming is affecting the dynamics and distribution limits of treeline ecotones worldwide (Greenwood and Jump, 2014; Korner, 2021), altering tree growth, phenology, and productivity (Hansson et al., 2021). Northern Russia, in particular, has experienced unprecedented warming in recent decades (Ciavarella et al., 2021; Overland and Wang, 2021; Rantanen et al., 2022), significantly exceeding the global mean (IPCC, 2023; Vinogradova et al., 2021) and reaching temperatures higher than in the past two to seven millennia (Esper et al., 2024; Hantemirov et al., 2022). Russian treelines are therefore ideal test frameworks to explore the skill of established and new temperature proxies and to study potentially non-stationary tree growth responses to changing climate.

Tree-ring width (TRW) and maximum latewood density (MXD) are commonly used high-resolution climate proxies (Esper et al., 2012, 2014; Kirdyanov et al., 2007; Rydval et al., 2015; Schneider et al., 2015; Schweingruber et al., 1978; Schweingruber, 1988;). TRW is particularly useful in temperature and water-limited environments (St. George, 2014) and has been extensively applied to reconstruct past climate variability, yielding detailed insights into historical climate patterns and trends (Büntgen et al., 2021; Esper et al., 2002; Fritts, 1976; Hantemirov et al., 2021, 2022; Hantemirov and Shiyatov, 2002). However, TRW-based temperature reconstructions may be affected by biological memory (Esper et al., 2015) and other external influences such as insect outbreaks (Barchenkov et al., 2023; 2007) diseases (Cherubini et al., 2002), and pollution (Kirdyanov et al., 2020). In contrast, MXD is less biased by non-climatic factors and, therefore, generally more suitable for dendroclimatic studies (Anchukaitis et al., 2013, 2017; Esper et al.,

* Corresponding author.
E-mail address: aarzac@gmail.com (A. Arzac).

https://doi.org/10.1016/j.dendro.2024.126267
Received 18 March 2024; Received in revised form 12 September 2024; Accepted 16 September 2024
Available online 17 September 2024

2002, 2016). MXD has been used for warm season temperature reconstructions in the Northern Hemisphere (Davi et al., 2003; Esper et al., 2010; Grudd, 2008), including Russia (Briffa et al., 2013; Schneider et al., 2015). Nevertheless, the methodology for producing MXD datasets is time-consuming, technically challenging, and expensive compared to TRW measurements (Björklund et al., 2019; Büntgen et al., 2007; Linderholm et al., 2010; Schweingruber, 1988; Zang and Biondi, 2013).

Latewood blue intensity (LWBI) and delta blue intensity (DBI) are gaining popularity in dendroclimatic studies as cost-effective surrogates for MXD, providing similar information (Björklund et al., 2019). Blue intensity (BI) refers to the inverted state of reflected light in the blue spectrum from an RGB digitized wood sample (Björklund et al., 2024), and DBI is the high-frequency difference between latewood and earlywood blue intensity (Björklund et al., 2014, 2024). These parameters have been widely used in North America (Babst et al., 2016; Heeter et al., 2021; Wilson et al., 2014, 2017) and Europe (Akhmetzyanov et al., 2020; Björklund et al., 2014, 2015; Frank and Nicolussi, 2020; Jiang et al., 2022; Reid and Wilson, 2020; Rydval et al., 2014; Seftigen et al., 2020) as proxies for temperature, drought and precipitation. However, less attention has been paid to Russia, with limited research in the Altai Mountains (Davi et al., 2021), central Siberia (Myglan et al., 2018), the White Sea (Semenyak and Dolgova, 2023) and Northern Caucasus (Dolgova, 2016).

In this study, we explore the dendroclimatological potential of LWBI and DBI measured in Siberian larch (*Larix sibirica* Ledeb.) from two temperature-limited upper treeline sites in the Ural Mountains, and compare these new data against TRW and MXD. The northern Ural Mountains, ranging from the Arctic tundra to temperate forests, are particularly suitable for dendroclimatic studies due to the severe temperature-limited conditions for growth (Devi et al., 2008; Hagedorn et al., 2014). Previous dendroclimatological studies based on TRW in the region provided valuable insights into historical climate variations, highlighting significant correlations between summer temperatures and tree growth (Briffa et al., 2013; Kukarskih et al., 2018; Pellizzari et al., 2017; Shyatov, 1986), particularly at the treeline (Gurskaya et al., 2012; Kukarskih et al., 2018; Vaganov et al., 1996), and linking upward vegetation shifts with increased winter precipitation (Devi et al., 2020; Hagedorn et al., 2014). Considering that density and blue intensity data from similar environments tend to exhibit strong temperature signals, we hypothesized that LWBI and DBI will strongly and positively respond to summer temperatures similar to MXD. We anticipate stronger signals in the Polar Urals due to its northernmost location and lower temperatures, highlighting the role of site-specific environmental conditions as driving factors of varying climate responses. We then discuss the relevance of LWBI and DBI as alternative temperature proxies in the region.

2. Methods

2.1. Study area and sampling design

Sixty uneven-aged Siberian larch trees were sampled at upper treeline sites in the Polar Urals (hereafter **PU**; 66°54'N, 65°45'E; 125 m a.s.l.) and the Northern Urals (hereafter **NU**; 59°37'N, 59°15'E; 750 m a.s.l.; Fig. 1a) during the summer of 2021. Wood cores were extracted at breast height using a 5-mm increment borer.

Mean annual temperature and total annual precipitation ranged from −5.8 °C to −0.2°C and from 450 mm to 850 mm at **PU** and **NU**, respectively, over the 1966–2020 period (Fig. 1b). Mean annual temperature has increased at rates of 0.55°C and 0.24 °C per decade at **PU** and **NU**, respectively, during the same period (Fig. 1c). Summer temperature (June-August) showed higher warming rates of 0.61°C and 0.34 °C per decade at **PU** and **NU**. In contrast, precipitation has not shown any significant trend. Meteorological data were obtained from

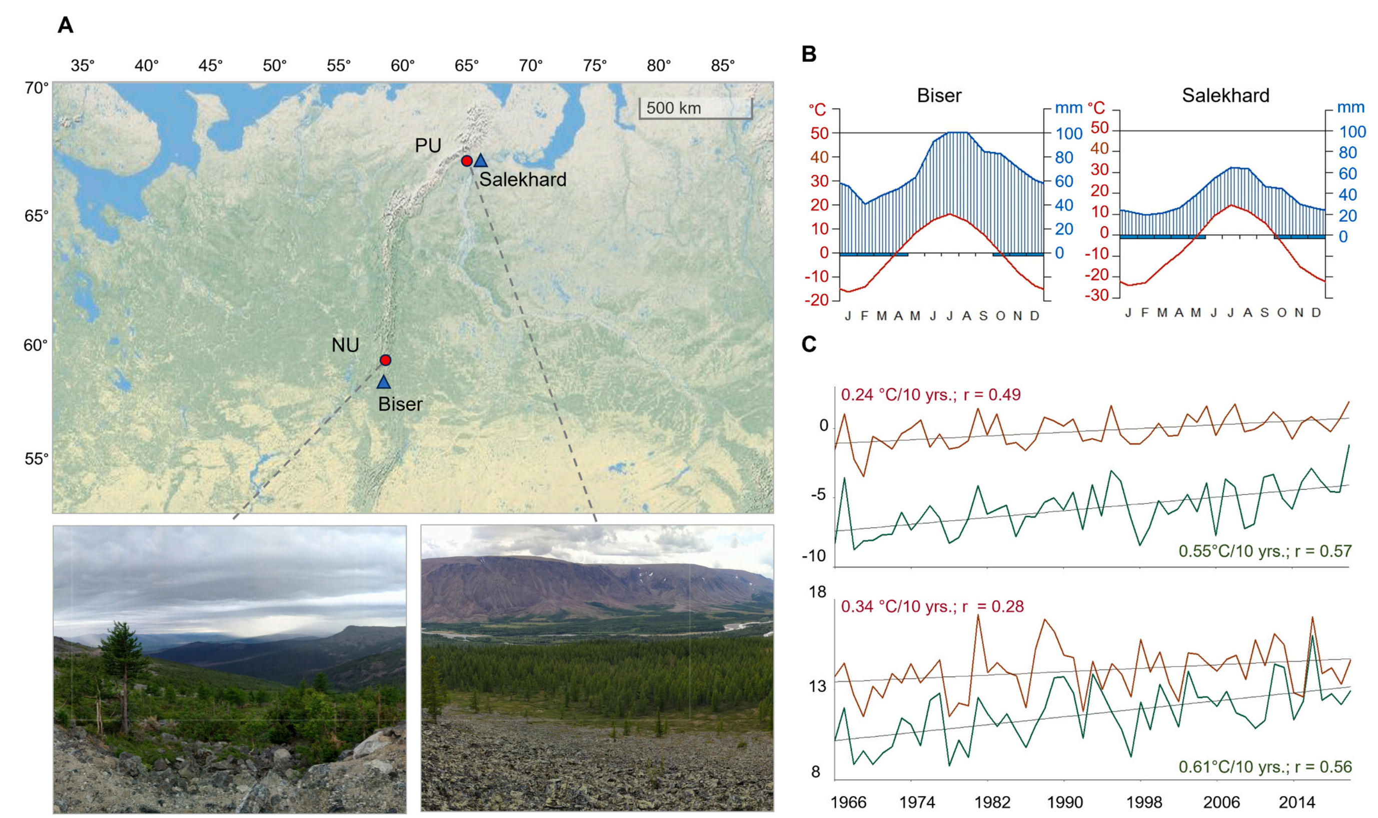

Fig. 1. Study sites and area. (A) The location of the sampling sites in the Polar Urals (PU) and Northern Ural (NU) is in red, and the nearby climate stations in Salekhard and Biser are in blue. (B) Biser and Salekhard climate diagrams over the 1966–2020 period. (C) Annual (upper panel) and June-August (lower panel) temperatures from 1966–2020 at Biser (red) and Salekhard (green).

https://www.meteo.ru from the nearest weather stations to each sampling site: Salekhard station (66°53'N, 66°53'E; 15 m a.s.l.), located approximately 50 km west of the **PU** site, and Biser station (58°51'N-58°87'E, 464 m a.s.l.), 86 km north of the **NU** site.

2.2. Tree-ring parameters and chronology development

Resin and organic substances were removed from the sampled cores using ethanol (96 %) for 72 hours (Cerrato et al., 2023) in a Soxhlet apparatus. This approach reduces the contrast between heartwood and sapwood (Rydval et al., 2014). The core samples were then submerged in water at 80°C for 48 hours to ensure extraction of remaining soluble substances. Afterward, the cores were air-dried and glued to wooden supports and polished with sandpaper up to 1200 grit. The polished cores were scanned at 3200 dpi using an Epson Perfection V800 flatbed scanner (Epson, Japan) calibrated with an IT8Calibration Target color card (Fuji) and interfaced with Silverfast SE software (LaserSoft Imaging, USA). The scanner was covered with a dark box to minimize external light interference (Rydval et al., 2014). TRW, earlywood width (EWW), latewood width (LWW) and BI measurements were performed using CooRecoder version 9.3 (Cybis Elektronik & Data AB, Sweden). DBI was calculated by subtracting earlywood blue intensity (EWBI) from latewood blue intensity (Björklund et al., 2014). The TRW series were visually cross-dated, and cross-dating was statistically verified with COFECHA (Grissino-Mayer, 2001). Due to wood discoloration issues, LWBI and DBI parameters were measured in only 23 and 22 trees at **PU** and **NU**, respectively.

All measurement series were standardized using a cubic-smoothing spline with a frequency response of 50 % at a wavelength of 2/3 of the series length in the "dplR" package (Bunn, 2008) in the R environment (R Core Team, 2022). TRW, EWW and LWW series were filtered using autoregressive modeling to remove autocorrelation and produce residual chronologies (Cook and Kairiukstis, 1990). The standardized series were combined using a robust biweight mean to create a standardized index chronology. The adjusted latewood index (LWadj) was derived by regressing EWW and LWW residual chronologies to remove the influence of earlywood (Meko and Baisan, 2001). The obtained mean chronologies were assessed using the expressed population signal (EPS), mean sensitivity (msx), mean inter-series correlation (r_{bt}) and the signal-to-noise ratio (SNR) (Wigley et al., 1984).

For comparison, previously produced MXD measurements (34 and 22 *L.* sibirica trees from the Polar and Northern Urals, respectively) were used to benchmark and compare climate signals in LWBI and DBI. MXD was measured according to the standard protocol (Schweingruber and Briffa, 1996), and the series detrended using 66 % splines in ARSTAN (Cook and Holmes, 1999) together with adaptive power transformation (Cook and Peters, 1997) applied prior to density trend removal.

2.3. Climate signal assessments

Pearson correlations were employed to assess the dependence of the measured parameters on climatic factors. Thus, TRW, EWW, LWadj, LWBI, DBI, and MXD standard chronologies were correlated against monthly temperature means, precipitation totals, and the Standardized Precipitation-Evaporation Index (SPEI, Vicente-Serrano et al., 2010) at different timescales (1–14 months). Additionally, to assess differences in the climate signals captured in the chronologies of the measured parameters, TRW, EWW, LWadj, LWBI and DBI residual chronologies were also correlated against detrended temperature and precipitation data. Correlations were performed from September of the previous year to September of the current year. The aggregated effect of climate parameters for consecutive months with the highest correlations in the current growing year (i.e., June-July and June-August) was also assessed. To estimate the stationarity of climate signals, 25-year running correlations were performed in the "Treeclim" package (Biondi and Waikul, 2004) in the R environment. Correlations for TRW, LWBI and DBI were calculated for the 1966–2020 period, whereas MXD was analyzed for the 1966–2001 period due to the length of the existing chronologies. Monthly climate data were obtained from the Federal Service for Hydrometeorology and Environmental Monitoring of the Russian Federation (https://www.meteo.ru) and SPEI data from The Spanish National Research Council (CSIC; https://spei.csic.es/index.html). Spatial correlation fields were computed in the KNMI Climate Explorer (https://climexp.knmi.nl/) using gridded 0.5×0.5° CRU TS 4.06 land temperatures.

3. Results

3.1. Tree growth and density measurements

TRW, LWBI, and DBI chronologies span 210 years (1811–2020) at both sites. The MXD chronologies, based on different sample sets, cover the1641–2001 (**PU**) and 1816–2003 (**NU**) periods, with mean series lengths of 361±105 and 188±34, respectively. TRW values range from 0.59±0.43 mm at **PU** to 0.99±0.69 mm at **NU**. Residual TRW chronologies (Fig. S1, raw series in Fig. S2) show higher mean sensitivity at **NU** than at **PU**. However, inter-series correlation and signal-to-noise ratio are higher at **PU** (Table 1). The r_{bt} values range from 0.65 to 0.68 for TRW, 0.36–0.56 for the blue intensity parameters, and 0.64–0.65 for MXD. TRW chronologies have a higher signal-to-noise ratio (SNR). The mean sensitivity (ms_x) for TRW is also significantly higher than for density parameters, indicating lower variability in density measurements compared to radial growth parameters. The Expressed Population Signal (EPS) is above 0.9 for all chronologies, confirming the reliability of the chronologies during the study period.

Pearson correlations between series show the strongest significant correlations between TRW and EWW ($r = 0.99$, 0.98; $P < 0.001$, at **PU** and **NU**, respectively), TRW and DBI ($r = 0.72$, 0.64; $P < 0.001$, at **PU** and **NU**, respectively), LWBI and DBI ($r = 0.87$, 0.91; $P < 0.001$, at **PU** and **NU**, respectively), and MXD with LWBI and DBI parameters (up to $r = 0.78$; $P < 0.001$, for MXD and DBI at **PU**) (Table S1).

3.2. Parameter-specific climate signals

Summer temperatures positively affect TRW- and BI-derived parameters at **PU** and **NU** during the 1966–2020, period and MXD during the shorter 1966–2001 period (Fig. 2). There are no significant changes in the timing and intensity of the climate signal in chronologies developed with different detrending methods (Tables S3 and S4). Therefore, only results for standard chronologies are presented. At **PU**, TRW and EWW are mainly influenced by June temperatures ($r = 0.51$ and 0.50, respectively; $P < 0.001$), and LWadj by July temperatures ($r = 0.44$; $P < 0.001$). The response strengthens with aggregated June-July

Table 1
Characteristics of the TRW, LWBI and DBI *Larix sibirica* chronologies for the 1966–2020 period and for the MXD for the 1966–2001 period.

	Parameter	ms_x	r_{bt}	EPS	SNR
Polar Urals	TRW	0.45	0.68	0.98	54.4
	EWW	0.49	0.68	0.98	54.3
	LWadj	0.43	0.57	0.97	34.5
	LWBI	0.14	0.36	0.93	13.8
	DBI	0.25	0.42	0.95	17.9
	MXD	0.15	0.64	0.98	24.5
Northern Urals	TRW	0.54	0.66	0.98	44.3
	EWW	0.58	0.66	0.98	44.3
	LWadj	0.56	0.62	0.97	37.4
	LWBI	0.19	0.56	0.97	27.8
	DBI	0.30	0.54	0.96	25.5
	MXD	0.13	0.65	0.97	17.6

ms_x = mean sensitivity, r_{bt} = mean inter-series correlation, EPS = expressed population signal, SNR = signal-to-noise ratio.

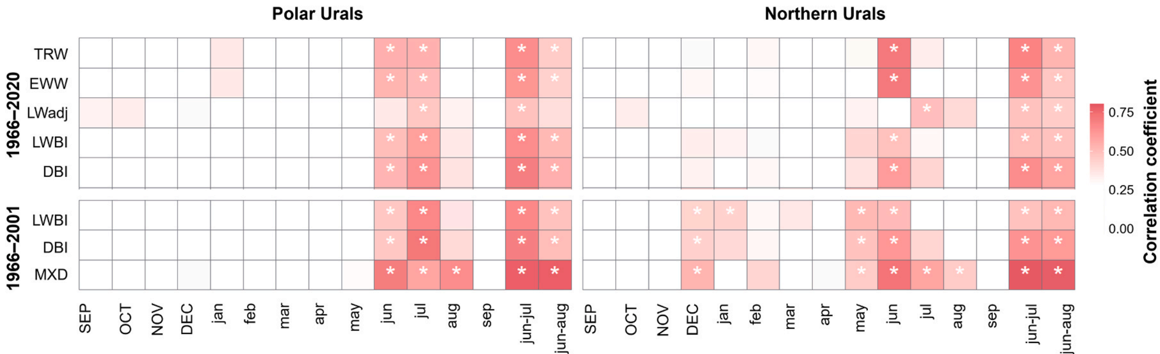

Fig. 2. Pearson correlations between tree-ring width (TRW), earlywood with (EWW), adjusted latewood (LWadj), latewood blue intensity (LWBI), delta blue intensity (DBI) and maximum latewood density (MXD) with mean monthly temperatures at the Polar and Northern Urals sites. Correlations were calculated from the previous year September (uppercase letters) to current-year September (lowercase letters), and the aggregated effect of June-July and June-August temperatures, over the 1966–2020 and 1966–2001 periods. All colored cells are significant at $P < 0.05$, and asterisks indicate correlations with $P < 0.01$.

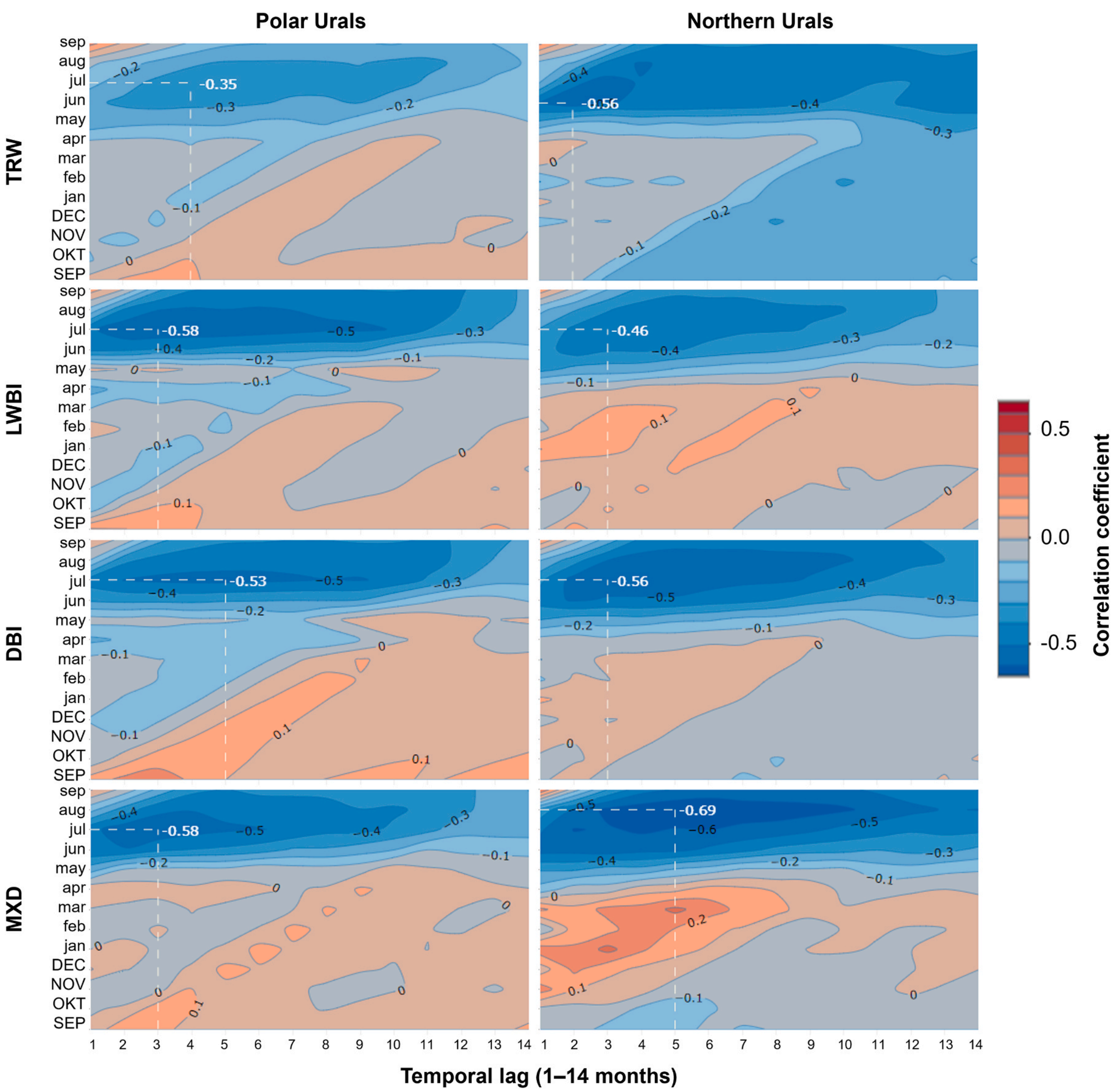

Fig. 3. Pearson correlations between tree-ring width (TRW), latewood blue intensity (LWBI), delta blue intensity (DBI) standard chronologies for the 1966–2020 period, and maximum latewood density (MXD, over the 1966–2001 period) with the monthly standardized precipitation–evaporation index (SPEI). Correlations were calculated from the previous year September (uppercase letters) to current-year September (lowercase letters) at different time lags (1–14 months). Dashed white lines show the month and time lag of the highest signal occurrence, with the correlation value indicated in white color. Correlation values (black color) above 0.22 and below −0.22 are significant for the period 1966–2020 ($P < 0.05$) and values above 0.28 and below −0.28 are significant for the period 1966–2001 ($P < 0.05$).

temperatures (r = 0.63, 0.61 and 0.45 for TRW, EWW and LWadj, respectively; $P < 0.001$). For LWBI and DBI, the maximal signal occurs in July (r = 0.57 and 0.62, respectively; $P < 0.001$), with a further increase of signal strength for June-July temperatures (r = 0.64 and 0.68, respectively; $P < 0.001$). MXD shows stronger signals from June to August, peaking in June and August (r = 0.68 and 0.64, respectively; $P < 0.001$). Correlations with seasonal temperature means for June-July and June-August are even higher (r = 0.77 and 0.78, respectively; $P < 0.001$).

At **NU**, temperature affects parameters earlier in the growing season, with a marginal but positive response to May temperatures. June temperature significantly influences most tree-ring parameters (r = 0.70, 0.69, 0.45 and 0.58 for TRW, EWW, LWBI, and DBI, respectively; $P < 0.001$). LWBI and DBI also correlate significantly with May temperatures (r = 0.37 and 0.33, respectively; $P < 0.05$), and LWadj responds to August temperatures (r = 0.40; $P < 0.05$). MXD shows more robust and prolonged temperature signals, particularly from May to August, peaking in June and July, r = 0.71 and 0.55, respectively ($P < 0.001$). The response of LWBI, DBI and MXD to aggregated June-July temperatures also increases (r = 0.47, 0.64 and 0.79, respectively; $P < 0.001$). Precipitation has significant but marginal ($P < 0.05$) negative effects at both sites, mainly in late spring and mid-summer (Fig. S3).

MXD shows stronger positive responses to summer temperatures than LWBI and DBI over the common 1966–2001 period (Fig. 2). The signal strength amplifies when considering the aggregated effect of temperature from consecutive months (June-July and June-August) at both sites. At **PU**, maximal LWBI and DBI signals occur in July (r = 0.65 and 0.70, respectively; $P < 0.001$), whereas the maximal MXD signal responds to the aggregated June-August temperatures (r = 0.78; $P < 0.001$). At **NU**, maximal LWBI and DBI signals also occur in July, but with lower signal intensity compared to **PU** (r = 0.48; $P < 0.01$ and 0.60, respectively), while MXD correlates the highest with the aggregated June-July temperatures (r = 0.78; $P < 0.001$). July precipitation negatively affects all the parameters at both sites, with stronger signals at **NU** (Fig. S3).

All parameters show significant negative correlations with SPEI at both sites (Fig. 3). At **PU**, the highest correlation values are found in July, with LWBI and MXD showing the strongest negative correlations (r= −0.58; $P < 0.001$) with a 3-month lag for both parameters, followed by DBI (r= −0.53; $P < 0.001$) with a 5-month lag, while TRW exhibits the weakest correlation (r= −0.35; $P < 0.01$). At **NU**, MXD shows the strongest negative correlation (r= −0.69; $P < 0.001$) in August with a 5-month lag, whereas LWBI shows the lowest correlation (r= −0.46; $P < 0.001$) in July with a 3-month lag. TRW and DBI mimic the intensity of the response (r= −0.56; $P < 0.001$), occurring in June (2- month lag) and July (3-month lag), respectively. When comparing between sites, TRW, DBI and MXD chronologies show lower signals at **PU** than **NU**, whereas LWBI signal is higher at **PU** than **NU**. EWW and LWadj responses to SPEI (Fig. S4) are lower at **PU** (r= −0.36 and −0.38; $P < 0.01$, with 3- and 2-month lags, respectively) than at **NU** (r= −0.51 and −0.57; $P < 0.001$, with 3- and 2-month lags, respectively).

3.3. Temporal and spatial stability of temperature signals

Running correlations between TRW, LWBI. DBI, and MXD standard chronologies show strong positive correlations with aggregated June-July and June-August temperatures at both sites, remaining significant ($P < 0.001$) over the entire period. MXD shows the highest correlation values compared to the other parameters at both sites (Fig. 4, please refer to Fig. S5 for individual monthly responses). At **PU**, LWBI, DBI, and MXD exhibit stronger temperature responses than TRW. Although correlations for all the parameters remain significant, TRW diverges from LWBI and DBI, with its temperature signal starting to decrease around 1996 (June-July) and 1993 (June-August). At **NU**, TRW response shifted over time compared to LWBI and DBI, showing a higher response to June-July temperatures from 1993 to 2002, while LWBI and DBI responses to June-August temperatures remain higher than TRW over the entire period. LWBI and DBI show a decline in the response to temperature around 1991, particularly pronounced for June-August temperatures.

Spatial correlation fields reaffirm the strong effect of aggregated June-July temperatures on TRW, LWBI, DBI, and MXD, with **PU** chronologies reaching stronger correlations than **NU** chronologies (Fig. 5). TRW and LWBI display the lower correlations at **PU** and **NU**, respectively, while MXD shows the strongest correlation compared to the other parameters at both sites over the shorter 1966–2001 period. The

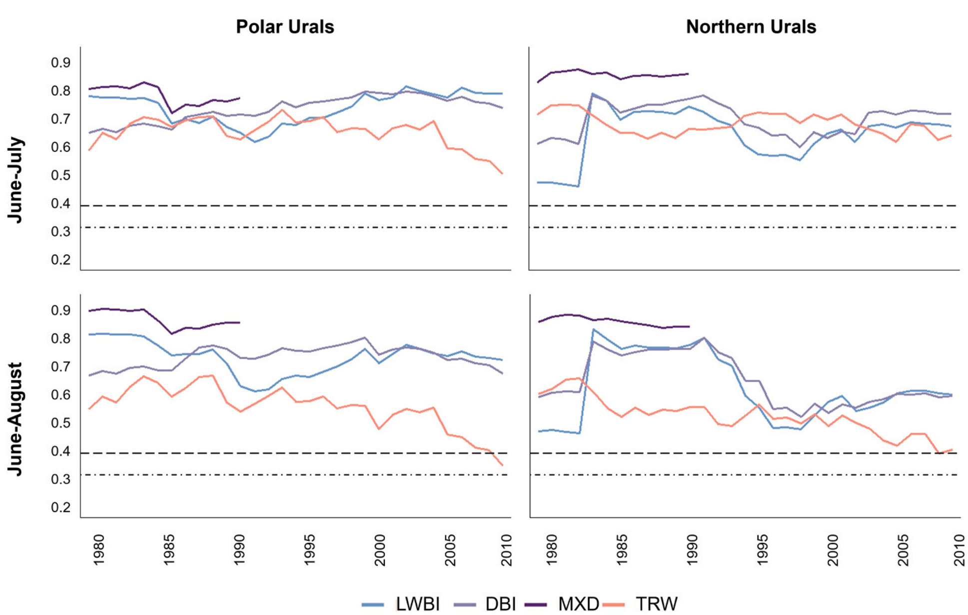

Fig. 4. 25-year running correlations of tree-ring width (TRW in orange), latewood blue intensity (LWBI in blue), delta blue intensity (DBI in light purple) standard chronologies against the aggregated June-July and June-August temperatures for the 1966–2020 period, and maximum latewood density (MXD in dark purple) for the 1966–2001 period. Dashed and dotted lines represent significant correlations at $P < 0.001$ and $P < 0.01$, respectively for the 1966–2020 period. The year refers to the middle of the 25-year window, shown every five years.

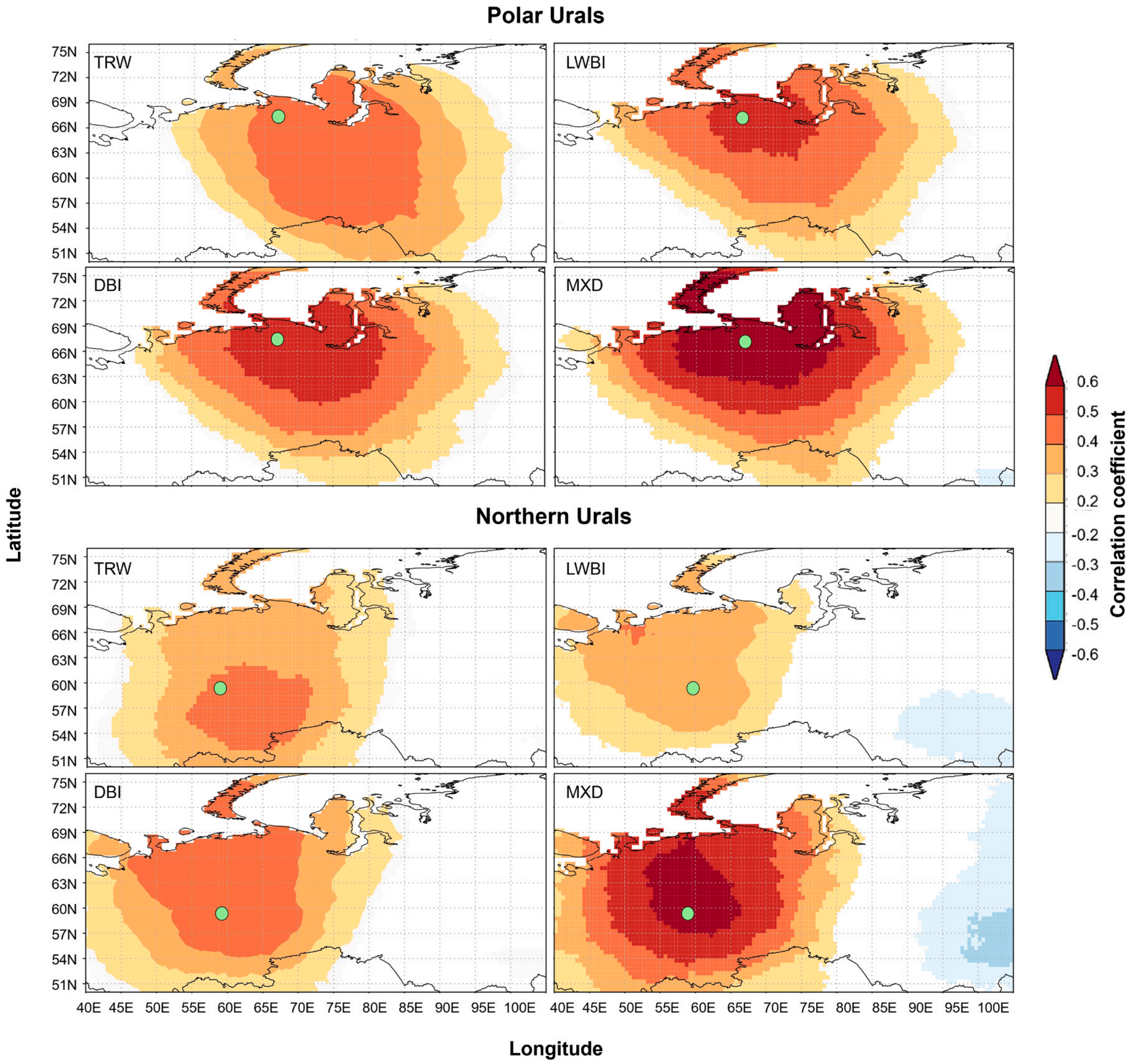

Fig. 5. Spatial field correlations between June-July mean temperatures (CRU TS 4.06, 0.5º) and tree-ring width (TRW), latewood blue intensity (LWBI), delta blue intensity (DBI) chronologies over the 1966–2020 period, and maximum latewood density (MXD) chronologies over the 1966–2001 period. Green points represent the location of sampling sites.

geographical coverage of the highest correlations for DBI ($r > 0.5$; 60º N–72º N, 60 º E–82º E) and MXD ($r > 0.6$; 63º N–72º N, 56 º E–80º E) at **PU** differs from that for the **NU** DBI ($r > 0.4$; 4º N–69º N, 46 º E–70º E) and MXD ($r > 0.6$; 57º N–69º N, 54 º E–65º E).

4. Discussion

Our exploration based on blue intensity parameters at upper tree line sites in the Ural Mountains has revealed, for the first time, a strong positive response of Siberian larch LWBI and DBI chronologies to summer temperatures, highlighting their potential as temperature proxies in the region. Differences in the timing and intensity of the temperature signals were observed between sites, with earlier and longer signals at **NU**, but generally weaker and less temporally robust compared to the northernmost site, **PU**. LWBI and DBI responses were slightly weaker than those of MXD, particularly at the southernmost site, **NU**.

Earlier (May) TRW responses to temperature at **NU** suggest milder growth conditions compared to **PU**, where lower temperatures (Table S2) delay tree growth onset to June. These temperature differences likely influence tree growth patterns and climate sensitivity, highlighting the adaptability of *L. sibirica* to varying conditions, similar to other conifers in central Siberia (Arzac et al., 2021a, 2021b; Henttonen et al., 2014). The relevance of site-specific conditions as a driving factor of climate response variability (e.g., Khotcinskaia et al., 2024; Kirdyanov et al., 2013) also affects the timing of BI and MXD maximal temperate signals between sites. Thus, **PU** shows generally more robust LWBI and DBI signals than **NU**, potentially due to stronger limitations by extremely low temperatures (Gurskaya et al., 2012; Kukarskih et al., 2018; Shyatov, 1986; Vaganov et al., 1996).

The temporal frame in which MXD, LWBI, and DBI encode temperature signals varies. MXD signals cover the entire growing season (Briffa et al., 1998; Büntgen et al., 2006; Kirdyanov et al., 2003), LWBI reflects temperature changes during a substantial part of the growing season (Rydval et al., 2014; Vyukhina and Gurskaya, 2022; Yue et al., 2023), and DBI spans a more extended period with higher intensity signal compared to LWBI (Björklund et al., 2021; Cerrato et al., 2023; Frank and Nicolussi, 2020; Fuentes et al., 2016; Seftigen et al., 2020; Wang et al., 2020; Wilson et al., 2014, 2017). Our results partially match the previous statement, showing a strong DBI temperature response compared to LWBI at both sites, but without differences in the timing they span. Moreover, our results align with previous studies in high-altitude regions of Western Mongolia, where DBI in Siberian larch showed a high correlation with June-July temperature compared to other parameters (Davi et al., 2021).

Our findings reveal a robust temporal sensitivity of MXD and BI-derived parameters to June-July temperatures at both sites. Sensitivity to June-August temperatures remains stable at **PU**, while at **NU**, it decreases, potentially due to increasing summer temperatures. TRW sensitivity to summer temperatures diverges from LWBI and DBI at **PU**, potentially signaling the "Divergence Problem" in the area (D'Arrigo et al., 2008). Significant correlations demonstrate a broad spatial coverage for LWBI, DBI, and MXD in the Ural Mountains, similar to patterns observed in Canada (Wang et al., 2020). Despite high correlation between MXD and BI-derived chronologies, aligned to previous studies (e.g., Kaczka et al., 2018), temperature responses are higher for MXD than LWBI and DBI. This difference may be due to biases from the lower resolution of BI measurements compared to MXD (Björklund et al., 2020, Wang et al., 2020), exacerbated by the narrowness of the rings in the study region. Unfortunately, limited literature on BI measurements for larch species and the absence of direct comparisons between BI-derived parameters and MXD for this species remain conspicuous.

Marginal negative precipitation signals at both sites, linked to a strong response to SPEI (Fig. 3), suggest no water limitation within the studied region, contrasting with the southern Urals Mountains (Agafonov et al., 2021; Khotcinskaia et al., 2024; Tabakova et al., 2020) and other regions of southern Siberia (Arzac et al., 2021b; Babushkina et al., 2017; Tabakova et al., 2020). On the contrary, extra soil moisture may negatively affect tree growth, as indicated by TRW negative response to May precipitations at both sites (Fig. S3). Warm May temperatures can lead to early snowmelt (Kirdyanov et al., 2003, Vaganov et al., 1999) providing extra water for growth, as well as potential access to water from thawing permafrost (Kirdyanov et al., 2024; Saurer et al., 2016; Sugimoto et al., 2002). At the same time, increased rainfall can also lead to waterlogging of permafrost areas (Gurskaya et al., 2012). Nevertheless, strong negative correlations with SPEI may be linked to collinearity with monthly temperatures, as is evidenced by significant negative correlations between SPEI and summer temperatures (Table S5).

Despite the potential of LWBI and DBI as temperature proxies in temperature-limited environments such as the Northern and Polar Urals, the current standard BI methodology has limitations. The response of MXD, and therefore BI-derived parameters, is determined by latewood cell size and cell wall dimensions (Björklund, et al., 2021; Silkin and Kirdyanov, 2003; Silkin et al., 2022), which are formed within a specific temperature range in Siberian larch (Vaganov et al., 1996). Under temperature-limited treeline conditions, where the growing season is extremely short (Bryukhanova et al., 2013; Rinne et al., 2015), cold spells can affect cell parameters (Vaganov et al., 1985; 1999), leading to the formation of narrow rings, latewood with a single cell row, or the occurrence of "blue" and "light" rings (Büntgen et al., 2022; Crivellaro and Büntgen, 2020; Filion et al., 1986; Piermattei et al., 2015). These conditions pose challenges for BI measurements due to the resolution limitations of commonly used flatbed scanner systems. Additionally, species with color discoloration issues, such as Siberian larch, may exhibit differences in contrast between heartwood and sapwood even after resin extraction, affecting the signal strength of BI parameters or necessitating the exclusion of collected material. Therefore, further development of BI methodologies, and new approaches based on high-resolution microscopy (Silkin et al., 2022; Rydval et al., 2024), are required to capture high-frequency variations and minimize the limitations of flatbed scanner systems.

5. Conclusion

The findings of this study support the use of latewood blue intensity and delta blue intensity as temperature proxies in temperature-limited northern and upper treeline environments along the Ural Mountains range. A detailed dendroclimatic analysis reveals novel blue intensity and classic MXD data from the Northen and Polar Ural to be closely coupled with temperature variations and contribute to our understanding of long-term climatic changes. Since the blue intensity methodology is much cheaper than X-ray-based MXD, it represents a valuable alternative to this established climate proxy. Future investigations encompassing a broader array of climatic parameters and tree species, as well as combined living-and-dead tree LWBI datasets, are required to further explore the skill to reconstruct low-frequency temperature variability in the region.

CRediT authorship contribution statement

Alberto Arzac: Writing – original draft, Methodology, Funding acquisition, Data curation, Conceptualization. **Vladimir Kukarskih:** Writing – review & editing, Methodology, Data curation. **Viktoria Agapova:** Writing – original draft, Methodology, Formal analysis, Data curation. **Alexander Kirdyanov:** Writing – review & editing, Conceptualization. **Ulf Büntgen:** Writing – review & editing, Conceptualization. **Jan Esper:** Writing – review & editing, Project administration.

Declaration of Competing Interest

The authors declare the following financial interests/personal relationships which may be considered as potential competing interests: Alberto Arzac reports financial support was provided by Ministry of Science and Higher Education of the Russian Federation. Vladimir Kukarskih reports financial support was provided by Basic Research Program of the Institute of Plant and Animal Ecology. Jan Esper reports financial support was provided by European Research Council. If there are other authors, they declare that they have no known competing financial interests or personal relationships that could have appeared to influence the work reported in this paper.

Data Availability

Data will be made available on request.

Acknowledgments

This work was carried out with the support of the Ministry of Science and Higher Education of the Russian Federation [FSRZ-2020–0014]. V. V.K was funded by the Basic Research Program of the Institute of Plant and Animal Ecology, Ural Branch of the Russian Academy of Sciences [122021000093–6]. U.B. and J.E. were funded by the ERC project MONOSTAR [AdG 882727]. We thank N. Devi and M. Bubnov for their support in the field.

Appendix A. Supporting information

Supplementary data associated with this article can be found in the online version at doi:10.1016/j.dendro.2024.126267.

References

Agafonov, L.I., Gurskaya, M.A., Kukarskih, V.V., Bubnov, M.O., Devi, N.M., Galimova, A. A., 2021. Insular pine forests of the Southern Urals and ribbon pine forests of the Altai as objects of dendroclimatic research. Russ. J. Ecol. 52, 349–357. https://doi.org/10.1134/S1067413621050039.

Akhmetzyanov, L., Sánchez-Salguero, R., García-González, I., Buras, A., DomínguezDelmás, M., Mohren, F., den Ouden, J., Sass-Klaassen, U., 2020. Towards a new approach for dendroprovenancing in the Mediterranean. Dendrochronologia 60. https://doi.org/10.1016/j.dendro.2020.125688.

Anchukaitis, K.J., D'Arrigo, R.D., Andreu-Hayles, L., Frank, D., Verstege, A., Curtis, A., Buckley, B.M., Jacoby, G.C., Cook, E.R., 2013. Tree-ring-reconstructed summer temperatures from Northwestern North America during the last nine centuries. J. Clim. 26, 3001–3012. https://doi.org/10.1175/JCLI-D-11-00139.1.

Anchukaitis, K.J., Wilson, R., Briffa, K.R., Büntgen, U., Cook, E.R., D'Arrigo, R., Davi, N., Esper, J., Frank, D., Gunnarson, B.E., Hegerl, G., Helama, S., Klesse, S., Krusic, P.J., Linderholm, H.W., Myglan, V., Osborn, T.J., Zhang, P., Rydval, M., Schneider, L., Schurer, A., Wiles, G., Zorita, E., 2017. Last millennium Northern Hemisphere summer temperatures from tree rings: Part II, spatially resolved reconstructions. Quat. Sci. Rev. 163, 1–22. https://doi.org/10.1016/j.quascirev.2017.02.020.

Arzac, A., Tabakova, M., Khotcinskaia, K., Koteneva, A., Kirdyanov, A., Olano, J., 2021b. Linking tree growth and intra-annual density fluctuations to climate in suppressed and dominant *Pinus sylvestris* L. trees in the forest-steppe of Southern Siberia. Dendrochronologia 67. https://doi.org/10.1016/j.dendro.2021.125842.

Arzac, A., Tychkov, I., Rubtsov, A., Tabakova, M.A., Brezhnev, R., Koshurnikova, N., Knorre, A., Buntgen, U., 2021a. Phenological shifts compensate warming-induced drought stress in southern Siberian Scots pines. Eur. J. For. Res. 140, 1487–1498. https://doi.org/10.1007/s10342-021-01412-w.

Babst, F., Wright, W.E., Szejner, P., Wells, L., Belmecheri, S., Monson, R.K., 2016. Blue intensity parameters derived from Ponderosa pine tree rings characterize intra-annual density fluctuations and reveal seasonally divergent water limitations. Trees 30, 1403–1415. https://doi.org/10.1016/j.dendro.2020.125688.

Babushkina, E., Belokopytova, L., Grachev, A., Meko, D., Vaganov, E., 2017. Variation of the hydrological regime of Bele-Shira closed basin in southern Siberia and its reflection in the radial growth of *Larix sibirica*. Reg. Environ. Chang. 17, 1725–1737. https://doi.org/10.1007/s10113-017-1137-1.

Barchenkov, A., Rubtsov, A., Safronova, I., Astapenko, S., Tabakova, K., Bogdanova, K., Anuev, E., Arzac, A., 2023. Features of Scots pine mortality due to incursion of pine bark beetles in symbiosis with ophiostomatoid fungi in the forest-steppe of Central Siberia. Forests 14 (7), 1301. https://doi.org/10.3390/f14071301.

Biondi, F., Waikul, K., 2004. DENDROCLIM2002: a C++ program for statistical calibration of climate signals in tree-ring chronologies. Comput. Geosci. 30, 303–311. https://doi.org/10.1016/j.cageo.2003.11.004.

Björklund, J., von Arx, G., Nievergelt, D., Wilson, R., Van den Bulcke, J., Günther, B., Loader, N.J., Rydval, M., Fonti, P., Scharnweber, T., Andreu-Hayles, L., Büntgen, U., D'Arrigo, R., Davi, N., De Mil, T., Esper, J., Gärtner, H., Geary, J., Gunnarson, B.E., Hartl, C., Hevia, A., Song, H., Janecka, K., Kaczka, R.J., Kirdyanov, A.V., Kochbeck, M., Liu, Y., Meko, M., Mundo, I., Nicolussi, K., Oelkers, R., Pichler, T., Sánchez-Salguero, R., Schneider, L., Schweingruber, F., Timonen, M., Trouet, V., Van Acker, J., Verstege, A., Villalba, R., Wilmking, M., Frank, D., 2019. Scientific merits and analytical challenges of tree-ring densitometry. Rev. Geophys. 57, 1224–1264. https://doi.org/10.1029/2019RG000642.

Björklund, J., Fonti, M.V., Fonti, P., Van den Bulcke, J., von Arx, G., 2021. Cell wall dimensions reign supreme: cell wall composition is irrelevant for the temperature signal of latewood density/blue intensity in Scots pine. Dendrochronologia 65. https://doi.org/10.1016/j.dendro.2020.125785.

Björklund, J.A., Gunnarson, B.E., Seftigen, K., Esper, J., Linderholm, H.W., 2014. Blue intensity and density from northern fennoscandian tree rings, exploring the potential to improve summer temperature reconstructions with earlywood information. Climate 10, 877–885. https://doi.org/10.5194/cp-10-877-2014.

Björklund, J., Gunnarson, B.E., Seftigen, K., Zhang, P., Linderholm, H.W., 2015. Using adjusted Blue Intensity data to attain high-quality summer temperature information: a case study from Central Scandinavia. Holocene 25, 547–556. https://doi.org/10.1177/0959683614562434.

Björklund, J., Seftigen, K., Fonti, P., Nievergelt, D., von Arx, G., 2020. Dendroclimatic potential of dendroanatomy in temperature-sensitive *Pinus sylvestris*. Dendrochronologia 60. https://doi.org/10.1016/j.dendro.2020.125673.

Björklund, J., Seftigen, K., Kaczka, R.J., Rydval, M., Wilson, R., 2024. A standard terminology for Blue Intensity (BI). Dendrochronologia 85. https://doi.org/10.1016/j.dendro.2024.126200.

Briffa, K.R., Melvin, T.M., Osborn, T., Hantemirov, R.M., Kirdyanov, A.V., Mazepa, V.S., Shiyatov, S.G., Esper, J., 2013. Reassessing the evidence for tree-growth and inferred temperature change during the Common Era in Yamalia, northwest Siberia. Quat. Sci. Rev. 72, 83–107. https://doi.org/10.1016/j.quascirev.2013.04.008.

Briffa, K.R., Schweingruber, F.H., Jones, P.D., Osborn, T.J., Harris, I.C., Shiyatov, S.G., Vaganov, E.A., Grudd, H., 1998. Trees tell of past climates: But are they speaking less clearly today? Philos. Trans. R. Soc. B Biol. Sci. 353, 65–73. https://doi.org/10.1098/rstb.1998.0191.

Bryukhanova, M.V., Kirdyanov, A.V., Propushkin, A.S., Silkin, P.P., 2013. Specific features of xylogenesis in Dahurian larch, *Larix gmelinii* (Rupr.) Rupr., growing on permafrost soils in Middle Siberia. Russ. J. Ecol. 44. https://doi.org/10.1134/S1067413613050044.

Bunn, A.G., 2008. A dendrochronology program library in R (dplR). Dendrochronologia 26, 115–124. https://doi.org/10.1016/j.dendro.2008.01.002.

Büntgen, U., Allen, K., Anchukaitis, K., Arseneault, D., Boucher, É., Bräuning, A., Chatterjee, S., Cherubini, P., Churakova, (Sidorova), O.V., Corona, C., Gennaretti, F., Grießinger, J., Guillet, S., Guiot, J., Gunnarson, B., Helama, S., Hochreuther, P., Hughes, M.K., Huybers, P., Kirdyanov, A.V., Krusic, P.J., Ludescher, J., Meier, W.J.-H., Myglan, V.S., Nicolussi, K., Oppenheimer, C., Reinig, F., Salzer, M.W., Seftigen, K., Stine, A.R., Stoffel, M., George, S.St, Tejedor, E., Trevino, A., Trouet, V., Wang, J., Wilson, R., Yang, B., Xu, G., Esper, J., 2021. The influence of decision-making in tree ring-based climate reconstructions. Nat. Commun. 12, 3411. https://doi.org/10.1038/s41467-021-23627-6.

Büntgen, U., Crivellaro, A., Arseneault, D., Baillie, M., Barclay, D., Bernabei, M., Bontadi, J., Boswijk, G., Brown, D., Christie, D.A., Churakova, O.V., Cook, E.R., D'Arrigo, R., Davi, N., Esper, J., Fonti, P., Greaves, G., Hantemirov, R.M., Hughes, M. K., Kirdyanov, A.V., Krusic, P.J., Le Quesne, C., Ljungqvist, F.C., McCormick, M., Myglan, V.S., Nicolussi, K., Oppenheimer, C., Palmer, J., Qin, C., Reinig, F., Salzer, M., Stoffel, M., Torbenson, M., Trnka, M., Villalba, R., Wiesenberg, N., Wiles, G., Yang, B., Piermattei, A., 2022. Global wood anatomical perspective on the onset of the Late Antique little Ice Age (LALIA) in the mid-6th century CE. Sci. Bull. 67 (22), 2336–2344. https://doi.org/10.1016/j.scib.2022.10.019.

Büntgen, U., Frank, D.C., Kaczka, R.J., Verstege, A., Zwijacz-Kozica, T., Esper, J., 2007. Growth responses to climate in a multi-species tree-ring network in the Western Carpathian Tatra Mountains, Poland and Slovakia. Tree Physiol. 27, 689–702. https://doi.org/10.1093/treephys/27.5.689.

Büntgen, U., Frank, D.C., Nievergelt, D., Esper, J., 2006. Summer temperature variations in the European Alps, A.D. 755-2004. J. Clim. 19, 5606–5623. https://doi.org/10.1175/JCLI3917.1.

Büntgen, U., Liebhold, A., Nievergelt, D., Wermelinger, B., Roques, A., Reinig, F., Krusic, P.J., Piermattei, A., Egli, S., Cherubini, P., Esper, J., 2020. Return of the moth: rethinking the effect of climate on insect outbreaks. Oecologia 192, 543–552. https://doi.org/10.1007/s00442-019-04585-9.

Cerrato, R., Salvatore, M.C., Carrer, M., Brunetti, M., Baroni, C., 2023. Blue intensity of Swiss stone pine as a high-frequency temperature proxy in the Alps. Eur. J. For. Res. https://doi.org/10.1007/s10342-023-01566-9.

Cherubini, P., Fontana, G., Rigling, D., Dobbertin, M., Brang, P., Innes, J.L., 2002. Tree-life history prior to death: two fungal root pathogens affect tree-ring growth differently. J. Ecol. 839–850. https://doi.org/10.1046/j.1365-2745.2002.00715.x.

Ciavarella, A., Cotterill, D., Stott, P., Kew, S., Philip, S., van Oldenborgh, G.J., Skålevåg, A., Lorenz, P., Robin, Y., Otto, F., Hauser, M., Seneviratne, S.I., Lehner, F., Zolina, O., 2021. Prolonged Siberian heat of 2020 almost impossible without human influence. Clim. Change 166, 9. https://doi.org/10.1007/s10584-021-03052-w.

Cook, E., Holmes, R., 1999. Chronology Development with Statistical analysis. USERS MANUAL for Program ARSTAN, Tucson, Arizona,USA.

Cook, E.R., Kairiukstis, L., 1990. Methods of Dendrochronology – Applications in the Environmental Sciences. Springer, Netherlands (Netherlands).

Cook, E.R., Peters, K., 1997. Calculating unbiased tree-ring indices for the study of climatic and environmental change. Holocene 7 (3), 361–370. https://doi.org/10.1177/095968369700700314.

Crivellaro, A., Büntgen, U., 2020. New evidence of thermally constrained plant cell wall lignification. Trends Plant Sci. 25 (4), 322–324. https://doi.org/10.1016/j.tplants.2020.01.011.

D'Arrigo, R., Wilson, R., Liepert, B., Cherubini, P., 2008. On the 'Divergence Problem' in Northern Forests: a review of the tree-ring 355 evidence and possible causes. Glob. Planet. Change 60. https://doi.org/10.1016/j.gloplacha.2007.03.004.

Davi, N.K., Jacoby, G.C., Wiles, G.C., 2003. Boreal temperature variability inferred from maximum latewood density and tree-ring data, Wrangell Mountain region. Alsk. Quat. Res. 60, 252–262. https://doi.org/10.1016/s0033-5894(03)00115-7.

Davi, N.K., Rao, M.P., Wilson, R., Andreu-Hayles, L., Oelkers, R., D'Arrigo, R., Nachin, B., Buckley, B., Pederson, N., Leland, C., Suran, B., 2021. Accelerated recent warming and temperature variability over the past eight centuries in the Central Asian Altai from blue intensity in tree rings. Geophys. Res. Lett. 48. https://doi.org/10.1029/2021GL092933.

Devi, N., Hagedorn, F., Moiseev, P., Bugmann, H., Shiyatov, S., Mazepa, V., Rigling, A., 2008. Expanding forests and changing growth forms of Siberian larch at the Polar Urals treeline during the 20th century. Glob. Chang. Biol. 14, 1581–1591. https://doi.org/10.1111/j.1365-2486.2008.01583.x.

Devi, N.M., Kukarskih, V.V., Galimova, A., Mazepa, V.S., Grigoriev, A.A., 2020. Climate change evidence in tree growth and stand productivity at the upper treeline ecotone in the Polar Ural Mountains. For. Ecosyst. 7. https://doi.org/10.1186/s40663-020-0216-9.

Dolgova, E., 2016. June-September temperature reconstruction in the Northern Caucasus based on blue intensity data. Dendrochronologia 39, 17–23. https://doi.org/10.1016/j.dendro.2016.03.002.

Esper, J., Büntgen, U., Frank, D.C., Nievergelt, D., Liebhold, A., 2007. 1200 years of regular outbreaks in alpine insects. Proc. R. Soc. B 274671–274679. https://doi.org/10.1098/rspb.2006.0191.

Esper, J., Cook, E.R., Schweingruber, F.H., 2002. Low-frequency signals in long tree-ring chronologies for reconstructing past temperature variability. Science 295, 2250–2253. https://doi.org/10.1126/science.1066208.

Esper, J., Düthorn, E., Krusic, P., Timonen, M., Büntgen, U., 2014. Northern European summer temperature variations over the Common Era from integrated tree-ring density records. J. Quat. Sci. 29, 487–494. https://doi.org/10.1002/jqs.2726.

Esper, J., Frank, D., Büntgen, U., Verstege, A., Hantemirov, R., Kirdyanov, A.V., 2010. Trends and uncertainties in Siberian indicators of 20th century warming. Glob. Chang. Biol. 16, 386–398. https://doi.org/10.1111/j.1365-2486.2009.01913.x.

Esper, J., Frank, D.C., Timonen, M., Zorita, E., Wilson, R.J.S., Luterbacher, J., Holzkämper, S., Fischer, N., Wagner, S., Nievergelt, D., Verstege, A., Büntgen, U., 2012. Orbital forcing of tree-ring data. Nat. Clim. Change 2, 862–866. https://doi.org/10.1038/nclimate1589.

Esper, J., Krusic, P.J., Ljungqvist, F.C., Luterbacher, J., Carrer, M., Cook, E., Davi, N.K., Hartl-Meier, C., Kirdyanov, A., Konter, O., Myglan, V., Timonen, M., Treydte, K., Trouet, V., Villalba, R., Yang, B., Büntgen, U., 2016. Ranking of tree-ring based temperature reconstructions of the past millennium. Quat. Sci. Rev. 145, 134–151. https://doi.org/10.1016/j.quascirev.2016.05.009.

Esper, J., Schneider, L., Smerdon, J.E., Schöne, B.R., Büntgen, U., 2015. Signals and memory in tree-ring width and density data. Dendrochronologia 35, 62–70. https://doi.org/10.1016/j.dendro.2015.07.001.

Esper, J., Torbenson, M., Büntgen, U., 2024. 2023 summer warmth unparalleled over the past 2,000 years. Nature 631. https://doi.org/10.1038/s41586-024-07512-y.

Filion, L., Payette, S., Gauthier, L., Boutin, Y., 1986. Light rings in subarctic conifers as a dendrochronological tool. (http://). Quat. Res. 26. https://doi.org/10.1016/0033-5894(86)90111-0.

Frank, T., Nicolussi, K., 2020. Testing different earlywood/latewood delimitations for the establishment of Blue Intensity data: a case study based on Alpine *Picea abies* samples. Dendrochronologia 64, 125775. https://doi.org/10.1016/j.dendro.2020.125775.

Fritts, H.C., 1976. Reconstructing spatial variations in climate. Tree Rings Clim. 434–505. https://doi.org/10.1016/b978-0-12-268450-0.50014-8.

Fuentes, M., Bjo rklund, J., Seftigen, K., Salo, R., Gunnarson, B.E., Linderholm, H.W., Aravena, J.C., 2016. A Comparison between Tree-ring Width and Blue Intensity High and Low Frequency Signals From *Pinus sylvestris* L. from the Central and Northern Scandinavian Mountains. STR16/04, 38.

Greenwood, S., Jump, A.S., 2014. Consequences of treeline shifts for the diversity and function of high altitude ecosystems. Arct., Antarct. Alp. Res. 46, 829–840. https://doi.org/10.1657/1938-4246-46.4.829.

Grissino-Mayer, H.D., 2001. Evaluating crossdating accuracy: a manual and tutorial for the computer program COFECHA. Tree-ring Res. 57 (2), 205–221.

Grudd, H., 2008. Torneträsk tree-ring width and density AD 500-2004: a test of climatic sensitivity and a new 1500-year reconstruction of north Fennoscandian summers. Clim. Dyn. 31, 843–857. https://doi.org/10.1016/j.dendro.2018.02.002.

Gurskaya, M., Hallinger, M., Singh, J., Agafonov, L., Wilmking, M., 2012. Temperature reconstruction in the Ob River valley based on ring widths of three coniferous tree species. Dendrochronologia 30, 302–309. https://doi.org/10.1016/j.dendro.2012.04.002.

Hagedorn, F., Shiyatov, S.G., Mazepa, V.S., Devi, N.M., Grigor'ev, A.A., Bartysh, A.A., Fomin, V.V., Kapralov, D.S., Terent'ev, M., Bugman, H., Rigling, A., Moiseev, P.A., 2014. Treeline advances along the Urals mountain range – driven by improved winter conditions? Glob. Chang. Biol. 20, 3530–3543. https://doi.org/10.1111/gcb.12613.

Hansson, A., Dargusch, P., Shulmeister, J., 2021. A review of modern treeline migration, the factors controlling it and the implications for carbon storage. J. Mt. Sci. 18, 291–306. https://doi.org/10.1007/s11629-020-6221-1.

Hantemirov, R.M., Corona, C., Guillet, S., Shiyatov, S.G., Stoffel, M., Osborn, T.J., Melvin, T.M., Gorlanova, L.A., Kukarskih, V.V., Surkov, A.Y., von Arx, G., Fonti, P., 2022. Current Siberian heating is unprecedented during the past seven millennia. Nat. Commun. 13, 1–8. https://doi.org/10.1038/s41467-022-32629-x.

Hantemirov, R.M., Shiyatov, S.G., Gorlanova, L.A., Kukarskih, V.V., Surkov, A.Y., Hamzin, I.R., Fonti, P., Wacker, L., 2021. An 8768-year Yamal tree-ring chronology as a tool for paleoecological reconstructions. Russ. J. Ecol. 52, 419–427. https://doi.org/10.1134/S1067413621050088.

Hantemirov, R.M., Shiyatov, S.G., 2002. A continuous-multimillennial ring-width chronology in Yamal, northwestern Siberia. Holocene 12, 717–726. https://doi.org/10.1191/0959683602hl585rp.

Harsch, M.A., Hulme, P.E., McGlone, M.S., Duncan, R.P., 2009. Are treelines advancing? A global meta-analysis of treeline response to climate warming. Ecol. Lett. 12, 1040–1049. https://doi.org/10.1111/j.1461-0248.2009.01355.x.

Heeter, K.J., Harley, G.L., Maxwell, J.T., Wilson, R.J., Abatzoglou, J.T., Rayback, S.A., Rochner, M.L., Kitchens, K.A., 2021. Summer temperature variability since 1730 CE across the low-to-mid latitudes of western North America from a tree ring blue intensity network. Quat. Sci. Rev. 267. https://doi.org/10.1016/j.quascirev.2021.107064.

Henttonen, H.M., Mäkinen, H., Heiskanen, J., Peltoniemi, M., Laurén, A., Hordo, M., 2014. Response of radial increment variation of Scots pine to temperature, precipitation and soil water content along a latitudinal gradient across Finland and Estonia. Agric. For. Meteorol. 198, 294–308. https://doi.org/10.1016/j.dendro.2019.125648.

Intergovernmental Panel on Climate Change (IPCC) (Ed.). 2023. Climate Change 2023: Synthesis report. Contribution of Working Groups I, II and III to the sixth assessment report of the Intergovernmental Panel on Climate Change. Geneva, Switzerland. https://doi.org/10.59327/IPCC/AR6-9789291691647.

Jiang, Y., Begović, K., Nogueira, J., Schurman, J., Svoboda, M., Rydval, M., 2022. Impact of disturbance signatures on tree ring width and blue intensity chronology structure and climatic signals in Carpathian Norway Spruce. Agric. For. Meteorol. 327. https://doi.org/10.1016/j.agrformet.2022.109236.

Kaczka, R.J., Spyt, B., Janecka, K., Beil, I., Büntgen, U., Scharnweber, T., Nievergelt, D., Wilmking, M., 2018. Different maximum latewood density and blue intensity measurements techniques reveal similar results. Dendrochronologia 49, 94–101. https://doi.org/10.1016/j.dendro.2018.03.005.

Khotcinskaia, K.I., Arzac, A., Kirdyanov, A.V., Tabakova, M., Olano, J.M., 2024. Constitutive resin ducts formation in *Pinus sylvestris* responds to water availability and temperature in southern Siberia. Agric. For. Meteorol. 347. https://doi.org/10.1016/j.agrformet.2024.109913.

Kirdyanov, A., Hughes, M., Vaganov, E., Schweingruber, F., Silkin, P., 2003. The importance of early summer temperature and date of snow melt for tree growth in the Siberian Subarctic. Trees – Struct. Funct. 17, 61–69. https://doi.org/10.1007/s00468-002-0209-z.

Kirdyanov, A.V., Krusic, P.J., Shishov, V.V., Vaganov, E.A., Fertikov, A.I., Myglan, V.S., Barinov, V.V., Browse, J., Esper, J., Ilyin, V.A., Knorre, A.A., Korets, M.A., Kukarskikh, V.V., Mashukov, D.A., Onuchin, A.A., Piermattei, A., Pimenov, A.V., Prokushkin, A.S., Ryzhkova, V.A., Shishikin, A.S., Smith, K.T., Taynik, A.V., Wild, M., Zorita, E., Büntgen, U., 2020. Ecological and conceptual consequences of Arctic pollution. Ecol. Lett. 23 (12), 1827–1837. https://doi.org/10.1111/ele.13611.

Kirdyanov, A.V., Propushkin, A.S., Tabakova, M.A., 2013. Tree-ring growth of Gmelin larch under contrasting local conditions in the north of Central Siberia. Dendrochronologia 31. https://doi.org/10.1016/j.dendro.2012.10.003.

Kirdyanov, A.V., Saurer, M., Arzac, A., Knorre, A.A., Prokushkin, A.S., Churakova (Sidorova), O.V., Arosio, T., Bebchuk, T., Siegwolf, R., Büntgen, U., 2024. Thawing permafrost can mitigate warming-induced drought stress in boreal forest trees. Sci. Total Environ. 912, 168858. https://doi.org/10.1016/j.scitotenv.2023.168858.

Kirdyanov, A.V., Vaganov, E.A., Hughes, M.K., 2007. Separating the climatic signal from tree-ring width and maximum latewood density records. Trees – Struct. Funct. 21, 37–44. https://doi.org/10.1007/s00468-006-0094-y.

Korner, C., 2021. The cold range limit of trees. Trends Ecol. Evol. 36, 979–989. https://doi.org/10.1016/j.tree.2021.06.011.

Körner, C., 2012. Alpine Treelines. Springer, Basel, p. 220. https://doi.org/10.1007/978-3-0348-0396-0.

Körner, C., Paulsen, J., 2004. A world-wide study of high altitude treeline temperatures. J. Biogeogr. 31, 713–732. https://doi.org/10.1111/j.1365-2699.2003.01043.x.

Kukarskih, V.V., Devi, N.M., Moiseev, P.A., Grigoriev, A.A., Bubnov, M.O., 2018. Latitudinal and temporal shifts in the radial growth-climate response of Siberian larch in the Polar Urals. J. Mt. Sci. 15, 722–729. https://doi.org/10.1007/s11629-017-4755-7.

Linderholm, H.W., Björklund, J.A., Seftigen, K., Gunnarson, B.E., Grudd, H., Jeong, J.H., Drobyshev, I., Liu, Y., 2010. Dendroclimatology in Fennoscandia – From past accomplishments to future potential. Clim 6, 93–114. https://doi.org/10.5194/cp-6-93-2010.

MacDonald, G.M., Kremenetski, K.V., Beilman, D.W., 2008. Climate change and the northern Russian treeline zone. Philos. Trans. R. Soc. B Biol. Sci. 363, 2285–2299. https://doi.org/10.1098/rstb.2007.2200.

Meko, D.M., Baisan, C.H., 2001. Pilot study of latewood-width of conifers as an indicator of variability of summer rainfall in the North American monsoon region. Int. J. Climatol. 21, 697–708. https://doi.org/10.1002/joc.646.

Myglan, V.S., Zharnikov, Z.Y., Sidorova, M.O., Barinov, V.V., Tainik, A.V., 2018. Application of the blue-intensity method for dating wooden buildings in Siberia. Archaeol. Ethnol. Anthropol. Eurasia 46, 109–113. https://doi.org/10.17746/1563-0102.2018.46.4.109-113.

Overland, J.E., Wang, M., 2021. The 2020 Siberian heat wave. Int. J. Climatol. 41, E2341–E2346. https://doi.org/10.1002/joc.6850.

Paulsen, J., Körner, C., 2014. A climate-based model to predict potential treeline position around the globe. Alp. Bot. 124, 1–12. https://doi.org/10.1007/s00035-014-0124-0.

Pellizzari, E., Camarero, J.J., Gazol, A., Granda, E., Shetti, R., Wilmking, M., Moiseev, P., Pividori, M., Carrer, M., 2017. Diverging shrub and tree growth from the Polar to the Mediterranean biomes across the European continent. Glob. Chang. Biol. 23, 3169–3180. https://doi.org/10.1111/gcb.13577.

Piermattei, A., Crivellaro, A., Carrer, M., Urbinati, C., 2015. The "blue ring": anatomy and formation hypothesis of a new tree-ring anomaly in conifers. Trees 29, 613–620. https://doi.org/10.1007/s00468-014-1107-x.

R Core Team, 2022. R: A Language and Environment for Statistical Computing. R foundation for statistical computing. ⟨https://www.r-project.org/⟩.

Rantanen, M., Karpechko, A.Y., Lipponen, A., Nordling, K., Hyvärinen, O., Ruosteenoja, K., Vihma, T., Laaksonen, A., 2022. The Arctic has warmed nearly four times faster than the globe since 1979. Commun. Earth Environ. 3. https://doi.org/10.1038/s43247-022-00498-3.

Reid, E., Wilson, R., 2020. Delta blue intensity vs. maximum density: a case study using *Pinus uncinata* in the Pyrenees. Dendrochronologia 61. https://doi.org/10.1016/j.dendro.2020.125706.

Rinne, K.T., Saurer, M., Kirdyanov, A.V., Bryukhanova, M.V., Prokushkin, A.S., Churakova (Sidorova), O.V., Siegwolf, R.T.W., 2015. Examining the response of needle carbohydrates from Siberian larch trees to climate using compound-specific δ13C and concentration analyses. Plant Cell Environ. 38. https://doi.org/10.1111/pce.12554.

Rydval, M., Björklund, J., von Arx, G., Begović, K., Lexa, M., Nogueira, J., Schurman, J. S., Jiang, Y., 2024. Ultra-high-resolution reflected-light imaging for dendrochronology. Dendrochronologia 83. https://doi.org/10.1016/j.dendro.2023.126160.

Rydval, M., Druckenbrod, D., Anchukaitis, K.J., Wilson, R., 2015. Detection and removal of disturbance trends in tree-ring series for dendroclimatology. Can. J. For. Res. 46, 387–401. https://doi.org/10.1139/cjfr-2015-0366.

Rydval, M., Larsson, L.Å., McGlynn, L., Gunnarson, B.E., Loader, N.J., Young, G.H.F., Wilson, R., 2014. Blue intensity for dendroclimatology: should we have the blues? Experiments from Scotland. Dendrochronologia 32, 191–204. https://doi.org/10.1016/j.dendro.2014.04.003.

Saurer, M., Kirdyanov, A.V., Prokushkin, A.S., Rinne, K.T., Siegwolf, R.T.W., 2016. The impact of an inverse climate–isotope relationship in soil water on the oxygen-isotope composition of Larix gmelinii in Siberia. N. Phytol. 209, 955–964. https://doi.org/10.1111/nph.13759.

Schneider, L., Smerdon, J.E., Büntgen, U., Wilson, R.J.S., Myglan, V.S., Kirdyanov, A.V., Esper, J., 2015. Revising midlatitude summer temperatures back to A.D. 600 based on a wood density network. Geophys. Res. Lett. 42, 4556–4562. https://doi.org/10.1002/2015GL063956.

Schweingruber, F.H., 1988. Tree Rings: Basics and Applications of Dendrochronology. Kluwer Academic Publishers, USA.

Schweingruber, F.H., Briffa, K.R., 1996. Tree-ring density networks for climate reconstruction. Last 2000 Years 43–66 Clim. Var. Forcing Mech.. https://doi.org/10.1007/978-3-642-61113-1_3.

Schweingruber, F., Fritts, H., Braker, O., Drew, L., Schar, E., 1978. The Xray technique as applied to dendroclimatology. Tree-ring Bull. 38, 61–91.

Seftigen, K., Fuentes, M., Ljungqvist, F.C., Björklund, J., 2020. Using Blue Intensity from drought-sensitive *Pinus sylvestris* in Fennoscandia to improve reconstruction of past hydroclimate variability. Clim. Dyn. 55, 579–594. https://doi.org/10.1007/s00382-020-05287-2.

Semenyak, N., Dolgova, E., 2023. Dendroclimatic Signals in the Pine and Spruce Chronologies in the Solovetsky Archipelago, Dendrochronologia 77, 126029. https://doi.org/10.1016/j.dendro.2022.126029.

Shyatov, S.G., 1986. Dendrochronology of highest line of forests in Ural. Science 136 (in Russian).

Silkin, P.P., Kirdyanov, A.V., 2003. The relationship between variability of cell wall mass of earlywood and latewood tracheids in larch tree-rings, the rate of tree-ring growth and climatic changes. Holzforschung 57 (1), 1–7. https://doi.org/10.1515/HF.2003.001.

Silkin, P.P., Kirdyanov, A.V., Krusic, P.J., Ekimov, M.V., Barinov, V.V., Büntgen, U., 2022. A new approach to measuring tree-ring density parameters. J. Sib. Fed. Univ. Biol. 15 (4), 441–455. https://doi.org/10.17516/1997-1389-0397.

St. George, S., 2014. An overview of tree-ring width records across the Northern Hemisphere. Quat. Sci. Rev. 95, 132–150. https://doi.org/10.1016/j.quascirev.2014.04.029.

Sugimoto, A., Yanagisawa, N., Naito, D., Fujita, N., Maximov, T.C., 2002. Importance of permafrost as a source of water for plants in east Siberian taiga. Ecol. Res. 17, 493–503. https://doi.org/10.1046/j.1440-1703.2002.00506.x.

Tabakova, M.A., Arzac, A., Martínez, E., Kirdyanov, A.V., 2020. Climatic factors controlling *Pinus sylvestris* radial growth along a transect of increasing continentality in southern Siberia. Dendrochronologia 62. https://doi.org/10.1016/j.dendro.2020.125709.

Vaganov, E.A., Shyatov S.G., Mazepa, V.S. 1996. Dendroclimatic research in the Ural-Siberian Subarctic. Nauka, Novosibirsk, Russia. (in Russian).

Vaganov, E.A., Hughes, M.K., Kirdyanov, A.V., Schweingruber, F.H., Silkin, P.P., 1999. Influence of snowfall and melt timing on tree growth in subarctic Eurasia. Nature 400, 149–151. https://doi.org/10.1038/22087.

Vaganov, E.A., Shashkin, A.V., Sviderskaya, I.V., Vysotskaya, L.G. 1985. Histometric Analysis of Woody Plant Growth. Nauka, Novosibirsk. (in Russian).

Vicente-Serrano, S.M., Beguería, S., López-Moreno, J.I., 2010. A multiscalar drought index sensitive to global warming: the standardized precipitation evapotranspiration index. J. Clim. 23, 1696–1718. https://doi.org/10.1175/2009JCLI2909.1.

Vinogradova, V., Titkova, T., Zolotokrylin, A., 2021. How climate change is affecting the transitional natural zones of the Northern and Arctic regions of Russia. Polar Sci. 29. https://doi.org/10.1016/j.polar.2021.100652.

Vyukhina, A.A., Gurskaya, M.A., 2022. Dendroclimatic potential of blue intensity-based chronologies of northern Fennoscandia Scots Pine. J. Sib. Fed. Univ. Biol. 15, 244–263. https://doi.org/10.17516/1997-1389-0385.

Wang, F., Arseneault, D., Boucher, É., Galipaud Gloaguen, G., Deharte, A., Yu, S., Trou-kechout, N., 2020. Temperature sensitivity of blue intensity, maximum latewood density, and ring width data of living black spruce trees in the eastern Canadian taiga. Dendrochronologia 64. https://doi.org/10.1016/j.dendro.2020.125771.

Wigley, T., Briffa, K., Jones, P., 1984. On the average value of correlated time series, with applications in dendroclimatology and hydrometeorology. J. Clim. Appl. Meteor. 23, 201–213. https://doi.org/10.1175/1520-0450(1984)023<0201:OTAVOC>2.0.CO;2.

Wilson, R., D'Arrigo, R., Andreu-Hayles, L., Oelkers, R., Wiles, G., Anchukaitis, K., Davi, N., 2017. Experiments based on blue intensity for reconstructing North Pacific temperatures along the Gulf of Alaska. Climate 13, 1007–1022. https://doi.org/10.5194/cp-13-1007-2017.

Wilson, R., Rao, R., Rydval, M., Wood, C., Larsson, L.Å., Luckman, B.H., 2014. Blue Intensity for dendroclimatology: The BC blues: a case study from British Columbia. Can. Holocene 24, 1428–1438. https://doi.org/10.1177/0959683614544051.

Yue, W., Seftigen, K., Chen, F., Wilson, R., Zhang, H., Miao, Y., Chen, Y., Zhao, X., 2023. *Picea schrenkiana* tree ring blue intensity reveal recent glacier mass loss in High Mountain Asia is unprecedented within the last four centuries. Glob. Planet. Change 228, 104210. https://doi.org/10.1016/j.gloplacha.2023.104210.

Zang, C., Biondi, F., 2013. Dendroclimatic calibration in R: the bootRes package for response and correlation function analysis. Dendrochronologia 31, 68–74. https://doi.org/10.1016/j.dendro.2012.08.001.